Measurement system for evaluation of the muon chambers for the LHCb experiment

Rafael A. Nóbrega [a],*, Davide Pinci [b]

[a] Universidade Federal de Juiz de Fora, Juiz de Fora, Brazil
[b] Istituto Nazionale di Fisica Nucleare, Rome, Italy

ABSTRACT

In a detector with the complexity of the LHCb, where only for the muon system more than 1300 chambers, divided into 20 different types, will be used, resulting on more than 120 k channels to be readout, it is of crucial importance to study the many types of chambers to create a complete knowledge of the detector operation and to guarantee a high-quality performance during the experiment. To make it possible, a complete setup was built and a C++ based software was developed to carry out a set of measurements on the full-equipped chambers of the LHCb muon detector. The setup is made of front-end control electronics, high-voltage supply and acquisition circuitry while the software, running on a PC, remotely controls each element of the system and implements a number of automatized procedures to assess the main characteristics of the chambers.

The main advantages of this system are its versatility and speed of measurement which are crucial to the experiment since there is the need to characterize every single chamber before final installation. Moreover, in this work it was proposed to measure the starting knee of the high-voltage operational plateau without the use of an external trigger by making use of the internal structure of the chambers. Two laboratories were prepared at CERN (European Laboratory for Particle Physics) to receive this system; one used to test chambers arrived from the CERN itself and the PNPI (Petersburg Nuclear Physics Institute) production sites, and one to test the chambers arrived from the INFN (National Institute of Nuclear Physics) production sites. In this document, the hardware and software setup will be presented together with the measurement-oriented implementations.

© 2011 Elsevier B.V. All rights reserved.

1. Introduction

The LHCb Muon Detector [1] is composed of five stations (M1–M5) and each station is divided into four regions (R1–R4). The inner most region (M1R1) is equipped with Triple Gas Electron Multiplier chambers (Triple-GEM) while all the other regions make use of Multi-Wired Proportional Chambers (MWPC) geometrically different depending on the station and region they are located. In total, 1368 MWPC, divided into 19 different types, and 24 GEM chambers are used. The chosen configuration leads to a detector geometry where the chamber type varies according to the distance and angle with respect to the collision point. The chambers' differences cause variations on their signal formation due to the different readout systems and pad dimensions. The LHCb system requires 99% efficiency for each chamber within a time window of 20 ns with a cluster size as low as 1.2. To cope with such requirements, the main chambers' operation parameters must be within certain limits as: the Equivalent Noise Charge (ENC) of each detector channel must be as low as 2 fC in order to have a high enough signal-to-noise ratio to achieve a muon detection efficiency higher than 99% for a chamber; threshold must be set in such a way that it keeps the noise rate of each channel low (e.g. 1 kHz) for trigger efficiency; chambers should present good uniformity between pads (e.g. $< 10\%$); high-voltage (HV) dark current must not be higher than few nA (e.g. < 10 nA) and the HV operation plateau must begin around 2450 V.

This document presents a system implemented to study the performance of the many LHCb muon chamber's types, able to perform automatized measurements by means of controlling the front-end, acquisition and high-voltage electronics; all controlled by a centralized software running on a local computer. The electronics setup and the software are introduced in Section 2 while the main implemented measurements are described in Section 3.

2. Acquisition system

2.1. Hardware

The main components of the acquisition setup is presented in Fig. 1. This system is able to acquire up to 10 full-equipped
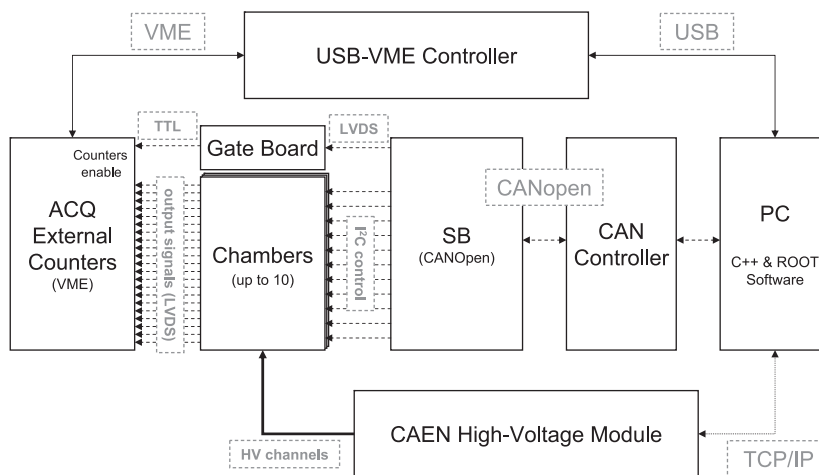
Fig. 1. Building block of the chamber control and acquisition system.

chambers in parallel. The readout system consists of front-end electronics (FEE) [2,3] and a VME FPGA-based circuitry (ACQ); used to process the LVDS signals generated by the FEE. Data-transfer between the ACQ board and the local computer is performed by a standard CAEN USB-VME controller. Front-end electronics features (e.g. threshold, delay and internal counters) are accessible via an LVDS-based I²C protocol implemented into the Service Board micro-controller firmware [4]. The communication between SB and the local computer is performed by means of the CANopen protocol. The system is compatible with two CAN controller devices, by Kvaser and by Systec, which are accessed via USB interface. The HV control implementation is compatible with the following CAEN devices: SY1527, SY2527LC and SY2527. To access the HV device it is used the TCP/IP protocol. Our setup can handle about 70 HV channels (40 are enough to equip 10 chambers). The HV modules can reach a value of 3000 V per channel while the operational HV range of the LHCb muon chambers goes up to 2800 V, with a working point around 2550 V.

2.2. Software and analysis

A Graphical User Interface software based on C++ and ROOT [5] has been developed to allow easy access and configuration of all the electronic devices being part of the system. A set of measurement procedures has been implemented as illustrated in the scheme of Fig. 2; the main features and measurements are explained along the Section 3. It provides real-time visualization during acquisition and, at the end of measurements, data are processed and shown in graphics to evidence the achieved results.

Between the available features, it has three specific panels to configure and check the following devices: FEE, the ACQ modules and the HV system. It also has a database where all the applied configurations and results can be archived.

3. Implemented measurements

Before starting the measurements, a chamber, or a set of them, must be connected to the system. It is done by connecting the I²C cables to the front-end boards and the HV channels to the gaps of the chamber(s). Once it is done, the software recognizes the I²C addresses of the front-end boards and carries out a charge injection procedure to assess the auto-injection circuitry and the input–output signal paths integrities. Then a set of measurements are available as shown on the scheme of Fig. 2. The main measurements are described in the next subsections.
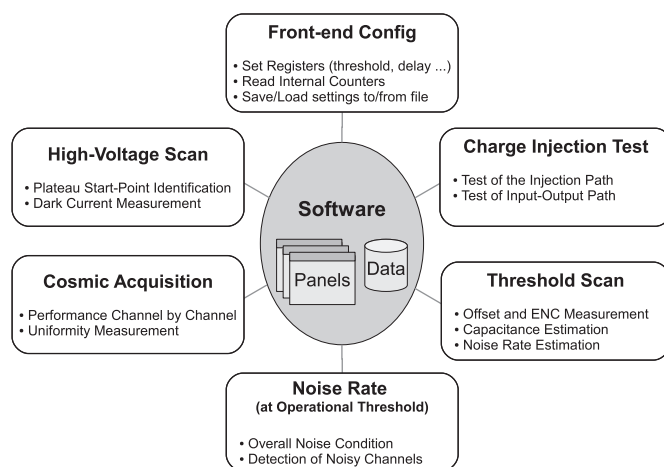

Fig. 2. Software scheme showing the implemented measurements.

3.1. ENC and offset

The ENC and the offset parameters of every single channel of the front-end electronics are estimated from the threshold scan procedure which is obtained by measuring the noise rate at the front-end channel's output for different threshold values, resulting in a curve relating the noise rate and the applied threshold as shown in Fig. 3.

The offset is determined by the threshold location where the highest rate is computed. With this method we have measured the offset spread of the LHCb muon front-end circuitry. As it can be seen in Fig. 4, the threshold can vary as much as 30 register units which is equivalent to approximately 70 mV. As an example, for the M5R4 chamber type, which has an estimated gain of 7 mV/fC, this value is equivalent to 10 fC showing that offset calibration is then mandatory for the LHCb muon system.

If the offset measured value is used to calibrate the threshold settings, a precision of ± 0.5 register is achieved (equivalent to ± 0.17 fC for the M5R4 chamber type which represents the worst case). Such a calibration permits to find the equivalent threshold in charge of the detector, to be compared with the average charge left by the passage of a muon particle, leading to an estimation of the channel efficiency.

The ENC measurement method consists of a gaussian fit to the threshold versus noise rate curve [6,7]. The precision of the ENC measurement has been estimated to be lower than 0.05 fC by

measuring many times the same channel in laboratory for different input capacitances (56, 100, 180 and 220 pF). In addition, the software applies a linear ENC-C_{det} conversion to estimate the chamber capacitance. Fig. 5 shows at left a histogram of the ENC measurement of five M4R4 chambers and at right a channel-by-channel plot of the capacitance estimation of a M4R4 chamber.

After measuring the offset and the ENC values, it is possible to obtain a threshold setting value $thr(fC)$ in terms of $n*ENC$. This value should then be translated in register units $thr(reg)$ to be written into the front-end Digital-to-Analog Converter (DAC) as follows:

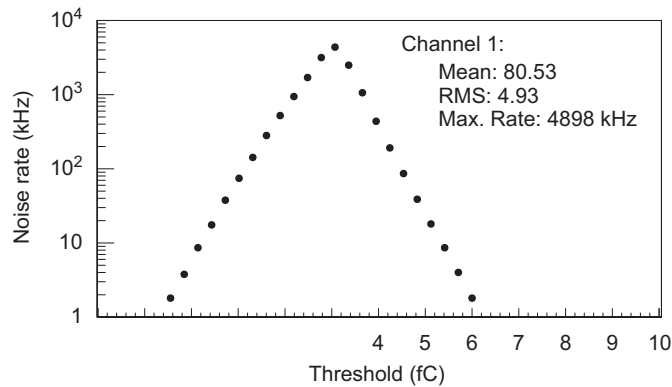$$thr(reg) = \frac{thr(fC)*A(mV/fC)}{2.35(mV/reg)} + B(reg) - C(reg) \qquad (1)$$

Fig. 3. Typical threshold scan measurement. In the program panel, the x axis can be shown in DAC register or charge units and the y axis in linear or log scale.
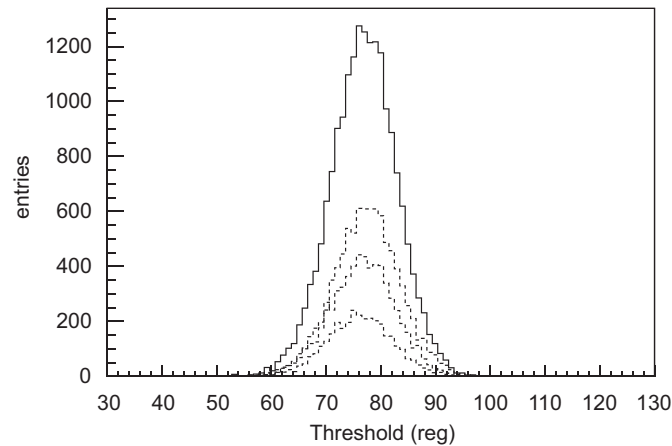

Fig. 4. Offset distribution of the FEE (18 800 channels) taken with the M5R4, M5R3 and M3R3 chamber types. The solid line histogram shows the sum of all measurements.
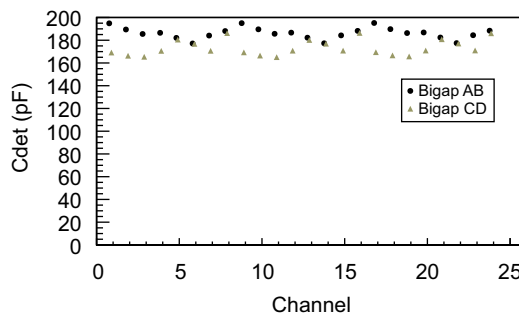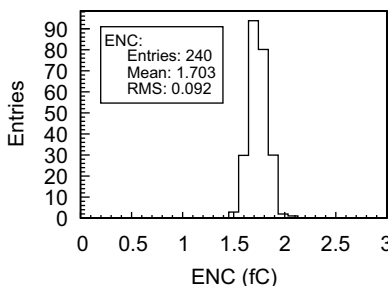
where A is the FEE sensitivity (mV/fC), which depends on the chamber's type, 2.35 mV/reg is the DAC resolution, B is the measured offset in register unit of the ASD threshold circuitry and C is the threshold bias which is related to the minimum measurable charge [8].

3.2. Noise rate estimation based on the threshold scan data

The software uses the threshold scan data and the Eq. (1) to estimate the noise rate for any given threshold. Fig. 6 shows the resulting noise rate distributions measured with 3024 channels of the M1R4 chamber's type. Two different threshold levels have been used: 4.9 fC (left plot) and 5.7 fC (right plot), which is equivalent to 6 and 7 sigmas, respectively, from the noise distribution center. At 4.9 fC, the noise rate mean value is of approximately 15 hits/s. All the chamber's types have been evaluated and it has been seen that a noise rate's mean value of about 10 hits/s leads to a noise rate's distribution where more than 99.8% of the channels have a noise rate below 1 kHz.

As an example, we estimated the threshold of several regions for a noise rate's mean value of approximately 10 hits/s; the result is shown in Table 1. Notice that the values reported here are not intended to be the final ones since some of the parameters involved in the calculation have been readjusted along the time. Nevertheless, the values of Table 1 are not far from recent values [9,10] from March and October 2010, respectively, with a standard deviation of the difference of about 0.5 fC. Notice that the standard deviation of the difference between the values presented in the Refs. [9,10] is of about 0.5 fC.

3.3. Noise rate at operational threshold

Measurement of the noise rate level at operational threshold of every channel is performed by reading out the front-end generated signals using either the FE internal counters or the ACQ external counters. The noise rate evolution can be visualized in real-time and statistical results are given at the end (values are calculated per chamber, per front-end and per bi-gap). Fig. 7 shows a noise rate measurement histogram of a M4R1 chamber after the first 9 s of acquisition for a threshold of 6 fC.

This measurement tests if the electronics noise rate of the chamber is under control, channel by channel. Noisy channels are detected in this stage and then replaced whenever needed. This procedure is also executed with the high-voltage on to detect pads with electric discharge. Usually, the counting rate of the channel under this effect is practically independent of the applied threshold, not requiring further data processing for its detection.

3.4. Cosmic acquisition

A specific cosmic acquisition procedure has been developed where an auto-triggering mode is used to reduce the background

Fig. 5. ENC measurement applied for five M4R4 chambers and capacitance estimation for one M4R4 chamber.
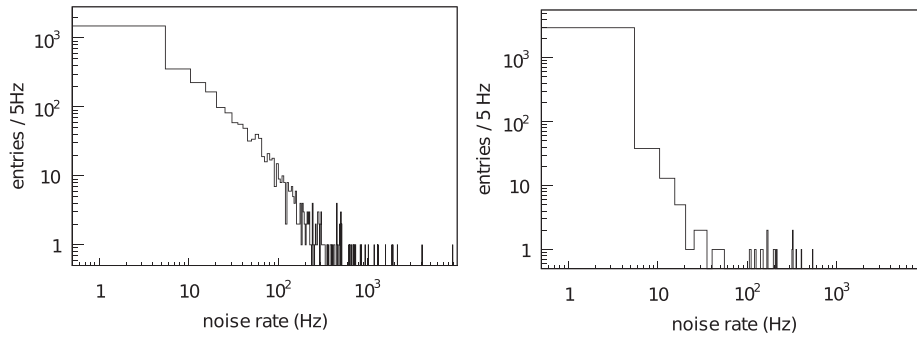
Fig. 6. Noise rate distribution using the threshold scan data of M1R4 chambers. The chamber-type related parameters used to set threshold are the gain (10.8 mV/fC) and the ENC (0.82 fC).

Table 1
Estimated threshold values for a noise rate mean value of about 10 hits/s.

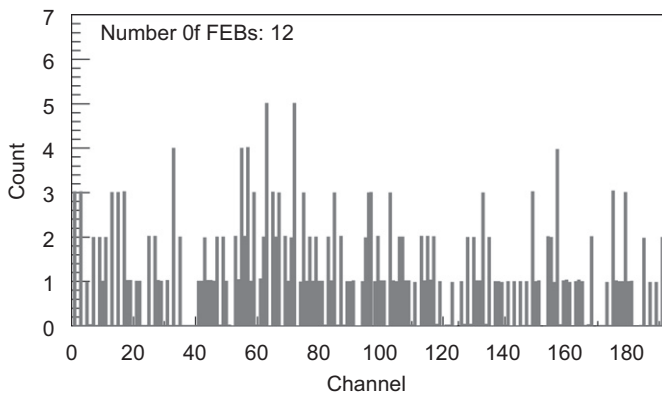| Chamber's type	Threshold (fC)	Chamber's type	Threshold (fC)	Chamber's type	Threshold (fC)
M1R1	–	M1R2	2.9	M1R3	3.0
M1R4	4.9	M2R1W	3.6	M2R1C	6.0
M2R2W	4.2	M2R2C	5.4	M2R3	5.3
M2R4	7.8	M3R1W	3.6	M3R1C	6.6
M3R2W	4.2	M3R2C	5.8	M3R3	5.4
M3R4	8.2	M4R1	4.2	M4R2	7.0
M4R3	7.2	M4R4	9.3	M5R1	4.4
M5R2	7.0	M5R3	7.4	M5R4	10.2

Fig. 7. Real-time acquisition: beginning of a noise rate measurement for a M4R1 chamber using the FEB internal counters (threshold set to 6 fC).

level. It requires a signal to be generated on the same xy coordinates by means of applying an AND between both MWPC bi-gaps in case of a quadri-gap chamber (see schematic of Fig. 8), or between single gaps for the chambers made of only two gaps. Such a setup permits to evaluate the performance of each single channel and to analyze the chamber's response uniformity according to the high-voltage and the threshold values (Section 3.4.1). A specific procedure has also been implemented to measure the counting rate and dark current for different HV values (Section 3.4.2).

3.4.1. Chamber response uniformity

By analyzing the cosmic rate of each channel and its distribution throughout the whole active area, it is possible to evaluate the chambers' response uniformity. This measurement is sensitive to efficiency and crosstalk pad-to-pad variations. Fig. 9 shows the resulting plot of the cosmic acquisition procedure applied to two

Fig. 8. Simplified scheme of a quadri-gap MWPC with wire readout.
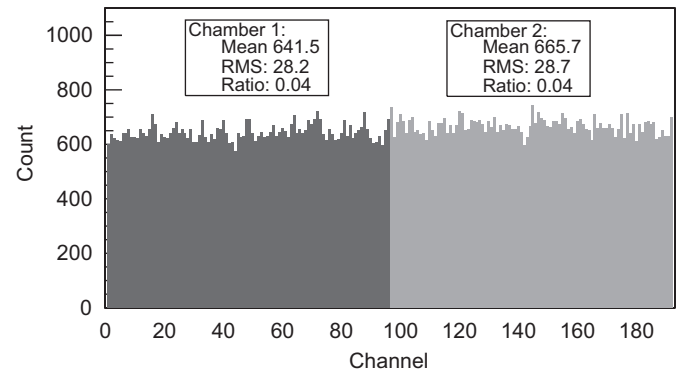

Fig. 9. Example of a cosmic rays acquisition real-time histogram for two M5R1 chambers in parallel. The HV was set to 2650 V and the threshold to 6 fC.

M5R1 chambers (sensitive area: 380×313 mm^2). Both chambers have presented an uniformity within 4% with a rate of 0.065 events/s per channel, resulting in a rate of about 50 events/s per m^2.

Fig. 10 shows a typical pad distribution after a cosmic rays acquisition run with a M3R1 chamber. The uniformity is better than 10%, considered, therefore, within the requirements.

3.4.2. Chamber HV plateau and dark current

The counting rate and the dark current are measured for different HV values in an automatic procedure. Those measurements are done with a HV channel per bi-gap (for chambers with four gaps) or per gap (for chambers with two gaps). During the measurement, one of the HV channel is fixed at the operational value while the other one is scanned. This measurement is used to compare the dark current and the counting rate evolution of both bi-gaps and to measure the beginning of the operational HV plateau.

Fig. 11 shows a typical measurement of a HV scan procedure applied to a M5R4 chamber: each data-point has been measured with an acquisition time of 480 s. The left plot shows the counting rate versus HV value; the start point of the plateau can be easily

determined by the knee which happens at about 2400 V. The knee is expected to be between 2300 and 2500 V depending on the chamber's type. It is also possible to see the point where the crosstalk starts increasing exponentially, at 2700 V. The right plot shows the dark current measurements; notice that while one of the HV channels is within the requirements, the other starts to increase rapidly at 2500 V, exceeding the dark current limit of 10 nA. Chambers with high values of dark current would be sent to a new HV training procedure [11].

To validate this measurement method, data has been taken with a full trigger system, using one scintillators below and one above a LHCb muon chamber. The chamber under test was of type M5R4 which presents the highest crosstalk level between gaps and, therefore, is the one most difficult to measure. The chamber total detection efficiency and the pad-cluster size have been studied with the chamber bi-gaps in logical AND. Data have been acquired in two different high-voltage configurations:

1. high voltage ON on the two bi-gaps;
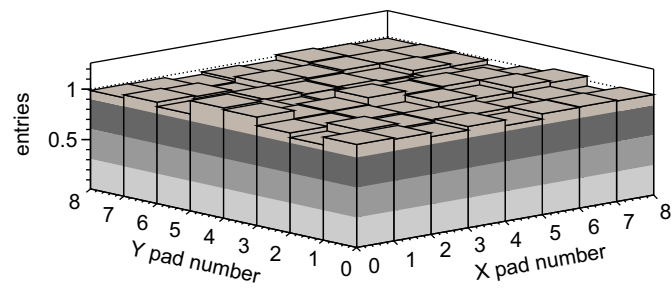2. one of the bi-gaps kept with high voltage OFF.

Fig. 10. Pad distribution normalized to its mean value (4714 ± 165), after a cosmic acquisition run with an M3R1 chamber (sensitive area: 332×273 mm^2).

In the latter case, without the crosstalk effect between gaps, no signals should be expected from the chamber. In configuration 1, the total detection efficiency plateau starts at 2550 V as it is shown in the left plot in Fig. 12. The detection efficiency in configuration 2 is entirely due to the crosstalk and it is found to be not completely negligible: 0.5% at 2650 V and 3.2% at 2800 V. The behavior of the average hit multiplicity (right plot in Fig. 12) shows a strong correlation between events with a high number of fired pads and events of crosstalk. In configuration 1, the probability of having multiplicity 1 is 91% while in configuration 2 it is only 26%.

In order to study the effect of the crosstalk on noise-induced hits we setup a random trigger acquisition with a rate of about 100 Hz. The trigger opens a gate of 500 μs in a multi-hit TDC. Duty cycle is about 5%. A run collecting 50 000 events corresponds to 25 effective seconds of data taking and lasts about 500 s. In the left plot of Fig. 13, the dependence on the high-voltage of the rate per pad measured with the random trigger method is compared with the one measured with the standard cosmic ray trigger. Both the bi-gaps of the chamber were high-voltage supplied. It is clear that up to 2600 V the two curves have the same behavior. The random trigger method makes possible to see the raise of the detection efficiency, the knee and the first part of the plateau where a rate of about 3 Hz per pad is reached. Starting from around 2600 V, the rate per pad shows a very fast increase. In order to understand where these hits come from, we studied the rate per pad with the random trigger in configuration 2. From the left plot in Fig. 12 we expect a low rate of hits due to cosmic rays: 0.06 Hz at 2700 V and 0.22 Hz at 2800 V. The measured rates, shown in the right plot of Fig. 13, are larger than the ones expected from the crosstalk of the cosmic ray tracks. Such a high rate can be explained as being due to the crosstalk of the chamber noise.

Fig. 14 shows that summing up the hits of the two single bi-gaps (right plot in Fig. 12) and the hits due to the cosmic rays
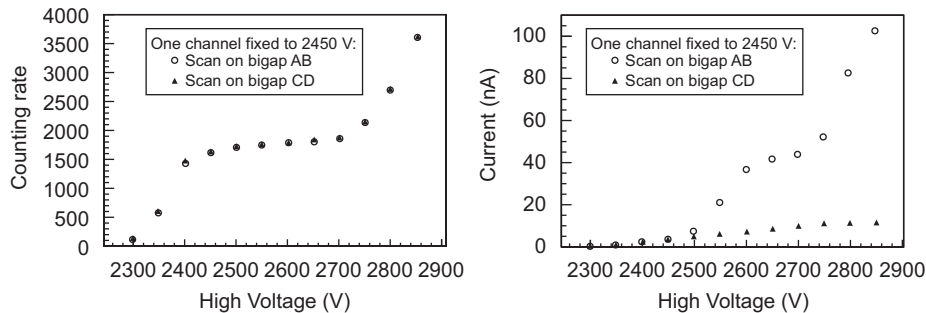

Fig. 11. Counting and dark current measurements performed during cosmic acquisition for a M5R4 chamber under the HV scan procedure. It is applied an AND logic combination between bi-gaps.
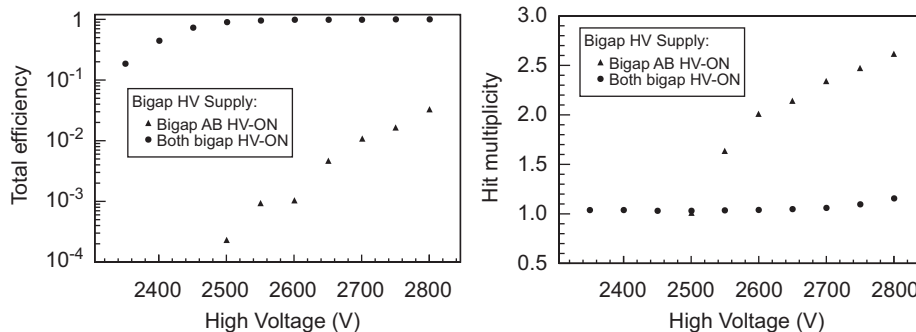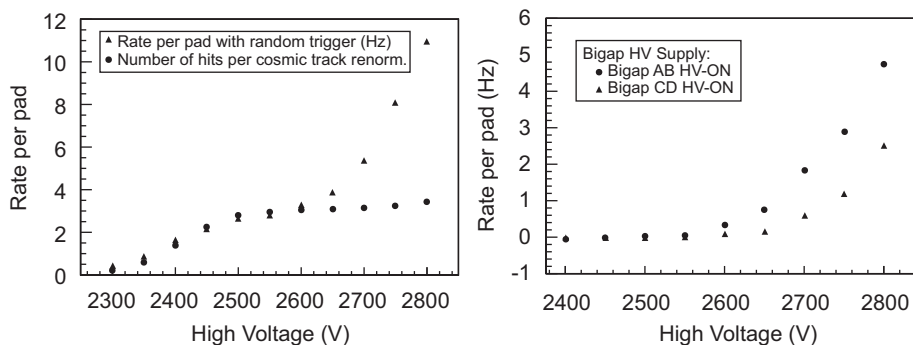

Fig. 12. At left it is shown the total detection efficiency in configuration 1 and 2 (see text). The right plot shows the chamber average number of hits per track detected with HV in both bi-gaps ON and with HV ON only in one bi-gap.

Fig. 13. At left it is shown the measured rate per pad with the random trigger method compared with the average number of hits per track. The second was rescaled to assume the same value of the first at 2450 V. The right plot shows the rate per pad with random trigger with only one bi-gap with HV ON.
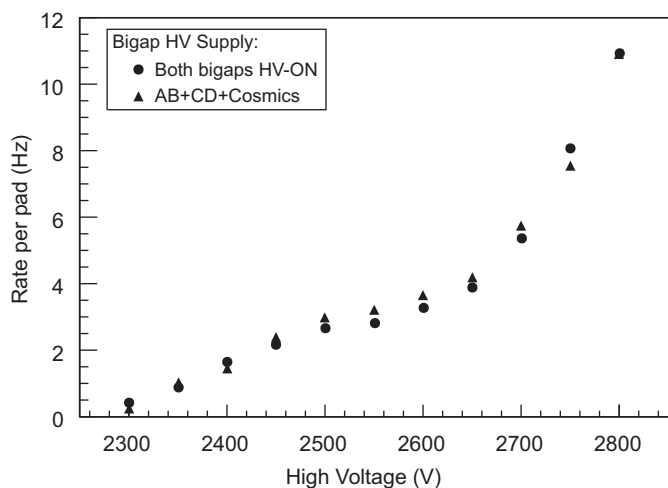

Fig. 14. Comparison between the hit rate measured in configuration 1 and the sum of the hits of the single bi-gaps and the hits due to the cosmic rays.

(circles on the left plot in Fig. 13) one obtains the rate measured with random trigger shown by the triangular data points on the left plot in Fig. 13. It demonstrates that a test performed without an external cosmic ray trigger and by setting the logical AND between the two bi-gaps is able to show the beginning of the chamber plateau but not the end of it because of the crosstalk between gaps.

4. Conclusion

This document has presented a measurement system developed to permit detailed studies and quality control of the LHCb Muon full-equipped chambers. All the installed chambers have been assessed by the presented system in order to minimize the problems encountered after the full assemblage of the detector. Tens of chambers had to be recovered because of problems

related to dead or noisy front-end channels. Some of the encountered problems were related to the HV operation, mostly because of high dark current or discharge between the chambers anode and cathode, and further HV conditioning was required. Few were the cases of pad-to-pad non-uniformity. The automatization of the measurements was fundamental to achieve a versatile, fast and, at the same time, robust system, making it possible to the experiment to assess the main operational characteristics of all the chambers before final installation. In addition, a method to measure the starting knee of the high-voltage operational plateau of the LHCb muon chambers without the use of an external trigger has been proposed. Measurements making use of an external trigger were carried out to demonstrate its validity.

References

[1] The LHCb Collaboration, Journal of Instrumentation 3 (2008) S08005.
[2] W. Bonivento, et al., Nuclear Instruments and Methods in Physics Research Section A 491 (1–2) (2002) 233.
[3] S. Cadeddu, et al., Nuclear Instruments and Methods in Physics Research Section A 518 (2004) 486.
[4] V. Bocci, et al., IEEE Transactions on Nuclear Science NS-57 (6) (2010).
[5] I. Antcheva, et al., Computer Physics Communications 180 (2009) 2499.
[6] S.O. Rice, Bell System Technical Journal 24 (1945) 46.
[7] H. Spieler, Electronics and Signal Processing, XI ICFA School on Instrumentation in Particle Physics, Bariloche, Argentina, January from 11 to 22, 2010.
[8] A. Kashchuk, et al., Procedure for determination and setting of thresholds implemented in the LHCb Muon system, CERN-LHCB-2008-052, 2008.
[9] L. Gruber, Optimization of the operating parameters of the LHCb muon system, Vienna University of Technology, Graduation Thesis, March 2010.
[10] D. Pinci, LHCb Muon Meeting, available online, 8th October 2010.
[11] M. Anelli, et al., IEEE Transactions on Nuclear Science NS-53 (1) (2006).